8. Seibyl J, Marek K, Quinlan D, et al. Decreased SPECT [^{123}I]β-CIT striatal uptake correlates with symptom severity in Parkinson's disease. *Ann Neurol* 1995;38:589–598.
9. Rinne J, Kuikka J, Bergstrom K, Rinne U. Striatal dopamine transporter in different disability stages of Parkinson's disease studied with [^{123}I]β-CIT SPECT. *Parkinsonism Relat Dis* 1995;1:47–51.
10. Marek K Seibyl J, Zoghbi S, et al. Iodine-123-β-CIT SPECT imaging demonstrates bilateral loss of dopamine transporters in hemi-parkinson's disease. *Neurology* 1996;46:231–237.
11. Seibyl J, Laruelle M, van Dyck C, et al. Reproducibility of [^{123}I]β-CIT SPECT brain measurement of dopamine transporters in healthy human subjects. *J Nucl Med* 1996;37:222–228.
12. Baldwin R, Zea-Ponce Y, Zoghbi S, et al. Evaluation of the monoamine uptake site ligand [^{123}I]methyl 3β-(4-iodophenyl)-tropane-2β-carboxylate (^{123}I)β-CIT in non-human primates: pharmacokinetics, biodistribution and SPECT brain imaging coregistered with MRI. *Nucl Med Biol* 1993;20:597–606.
13. Langston J, Widner H, Goetz CG, et al. Core assessment program for intracerebral transplantations. *Mov Dis* 1992;7:2–13.
14. Fahn S, Elton R, Members of the UPDRS Development Committee Unified Parkinson's disease rating scale. In: Fahn S, Marsen CD, Calne DB, Goldstein M, eds. *Recent developments in Parkinson's disease*, vol. 2. Florham Park, NJ: Macmillan Healthcare Information; 1987:153–164.
15. Chang LT. A method for attenuation correction in computed tomography. *IEEE Trans Nucl Sci* 1987;NS-25:638–643.
16. LeWitt PA. Clinical trials of neuroprotection in Parkinson's disease: long-term selegiline and alpha-tocopherol treatment. *J Neural Trans Suppl* 1994;43:171–181.
17. Lee C, Schulzer M, Mak E, et al. Clinical observations on the rate of progression of idiopathic parkinsonism. *Brain* 1994;117:501–507.
18. Morrish P, Sawle G, Brooks D. An [^{18}F]dopa-PET and clinical study of the rate of progression in Parkinson's disease. *Brain* 1996:in press.
19. Vingerhoets F, Snow B, Lee C, Schulzer M, Mak E, Calne D. Longitudinal fluorodopa positron emission tomographic studies of the evolution of idiopathic parkinsonism. *Ann Neurol* 1994;36:759–764.

Regional Methionine and Glucose Uptake in High-Grade Gliomas: A Comparative Study on PET-Guided Stereotactic Biopsy

Serge Goldman, Marc Levivier, Benoît Pirotte, Jean-Marie Brucher, David Wikler, Philippe Damhaut, Sophie Dethy, Jacques Brotchi and Jerzy Hildebrand

PET/Biomedical Cyclotron Unit, Service de Neurologie and Service de Neurochirurgie, ULB-Hôpital Erasme; and Department of Neuropathology, Cliniques Universitaires Saint-Luc, Brussels, Belgium

Gliomas are regionally heterogeneous tumors. The local relationship between histologic features and radiotracer uptake evaluated by PET should therefore influence analysis and interpretation of PET results on gliomas. This study explored this local relationship as a result of PET guidance of stereotactic biopsies. **Methods:** Local histology was confronted to the regional uptake of ^{18}F-2-fluoro-2-deoxy-D-glucose (^{18}F-FDG) and ^{11}C-methionine (^{11}C-MET) in 14 patients with high-grade glioma diagnosed during a procedure of PET-guided stereotactic biopsies. We analyzed the uptake of both tracers in regions of interest centered on the stereotactic coordinates of 93 biopsy samples. **Results:** A semiquantitative analysis revealed a significant regional correlation between ^{11}C-MET and ^{18}F-FDG uptakes. Uptake of both tracers was significantly higher on the site of tumor samples showing anaplastic changes than in the rest of the tumor. Presence of necrosis in anaplastic areas of the tumor significantly reduced the uptake of ^{11}C-MET. **Conclusion:** PET with ^{11}C-MET and ^{18}F-FDG may help to evaluate, in vivo, the metabolic heterogeneity of human gliomas. Anaplasia is a factor of increased uptake of both tracers, but microscopic necrosis in anaplastic areas influences their uptake differently. This finding probably relates to the differences in tracer uptake by non-neoplastic components of necrotic tumors. These results underline the complementary role of ^{18}F-FDG and ^{11}C-MET for the study of brain tumors and favors their use for stereotactic PET guidance of diagnostic or therapeutic procedures.

Key Words: glioma; PET; fluorine-18-fluorodeoxyglucose; methionine; stereotaxy

J Nucl Med 1997; 38:1459–1462

Different radiotracers have been used with PET to help in the management of patients with glioma (*1,2*). These tracers may be classified into three groups: the markers of energetic metabolic pathways, the markers of protein and nucleic acid synthetic pathways and the radioligands for receptor imaging. Most investigators use tracers from the two first classes, e.g., ^{18}F-2-fluoro-2-deoxy-D-glucose (^{18}F-FDG) which assays glucose metabolism, and ^{11}C-methionine (^{11}C-MET) or other amino acid tracers, which assay amino acid transport and metabolism (*3–7*). Tracer choice depends on the goals pursued which may involve diagnosis, lesion delineation, grade and prognosis estimation and evaluation or prediction of response to treatment. For instance, it has been claimed that, for the definition of tumor limits, PET with ^{11}C-MET (MET-PET) is better than PET with ^{18}F-FDG (FDG-PET) or other modalities such as CT and MRI (*8,9*). To compare the characteristics of different PET tracers, it is essential to ascertain that the brain regions investigated during different PET procedures are similar, a condition which may be fulfilled using matching (*10*) or preferably stereotactic methods (*8,11–13*). Another important requisite for these comparative analyses is the definition, on the brain images, of regions of interest (ROIs) which adequately sample the tumor tissue. Since areas of high tracer uptake may be different with diverse tracers and since other imaging modalities, such as MRI, cannot ensure where the limits of the tumor are (*9*), histologic control of the regions concerned by the analysis seem to offer the best guarantee that this requirement is achieved. Furthermore, this histologic control allows confrontation of the multiple metabolic data with pathological features of the tumor. Therefore, we decided to apply a procedure of PET-guided stereotactic biopsies (*11*) to the comparison and histologic confrontation of PET information provided by two major tumor tracers used for the management of brain tumors: ^{18}F-FDG and ^{11}C-MET.

MATERIALS AND METHODS

Patients

A consecutive series of 19 patients suspected of having a brain tumor gave informed consent to undergo stereotactic biopsies guided by CT and by PET with successive injection of ^{11}C-MET and ^{18}F-FDG after a procedure which allows image data acquisi-

Received Jan. 22, 1996; revision accepted Jul. 22, 1996.
For correspondence or reprints contact: Serge Goldman, MD, PET/Biomedical Cyclotron Unit, ULB-Hôpital Erasme, 808, route de Lennik, B-1070 Brussels, Belgium.

TABLE 1
Patient Characteristics

Patient no.	Age (yr)	Gender	No. of samples	Location of lesion	Diagnosis
1	60	M	4	Left parietal	GB
2	66	M	5	Right frontotemporal	GB
3	54	M	7	Right thalamus	AA
4	50	F	5	Right frontal	AA
5	68	F	9	Right frontal	GB
6	75	M	5	Left lenticular	GB
7	32	M	4	Right frontal	AA
8	63	F	5	Left frontoparietal	GB
9	71	M	4	Left temporoparietal	GB
10	47	M	8	Right parietal	AA
11	61	M	10	Left frontal	AA
12	32	F	8	Right thalamus	AA
13	56	M	10	Right thalamolenticular	GB
14	61	M	9	Left temporal	OA

AA = anaplastic astrocytoma; OA = anaplastic oligodendroglioma; GB = glioblastoma.

tion (stereotactic CT and PET), surgical planning and biopsies on the same day, as described in detail elsewhere (*11*). The analysis was conducted on 14 patients with a diagnosis of high-grade glioma (Table 1). Diagnosis in the patients not included in the analysis was low-grade astrocytoma (n = 1), metastasis from undifferentiated tumor (n = 2), gliosis from undetermined origin (n = 1) and vascular lesion (n = 1).

In all patients, we obtained the PET scans (15 6.75-mm-thick adjacent slices, eight direct and seven crossed slices, covered the entire brain) in stereotactic conditions after a protocol previously described (*11,14*). The patients were fasted, conscious, in a supine resting state with eyes closed and ears unplugged. The in-plane spatial resolution (FWHM) was about 5 mm. During PET acquisition, the stereotactic head-ring was secured to the clamp, which fits both into the CT and into the PET couch. The fiducial reference system used for stereotactic PET consisted of V-shape tubing filled with an ^{18}F-fluoride solution adapted on four localization plates originally designed for stereotactic MRI. Before the emission scans, a transmission scan was obtained using a ring source filled with an ^{18}F-fluoride solution and allowing a measured correction of the images for attenuation. The subjects were first injected intravenously with a bolus of 370–550 MBq (10–15 mCi) ^{11}C-MET prepared with an automated synthesis system after the procedure described by Comar et al. (*15,16*), and an image was acquired from 20–40 min postinjection. At least 80 min after the ^{11}C-MET injection, each patient was injected with a bolus of about 260 MBq (7 mCi) ^{18}F-FDG prepared after the method of Hamacher et al. (*17*). The delay between both injections ensured negligible contamination of the PET-FDG images by residual ^{11}C radioactivity. Static PET-FDG images were acquired from 40–60 min postinjection.

To estimate the radioactive content at the level of each biopsy sample site, circular 0.3 cm^2 ROIs were centered on the coordinates of the actual biopsy recorded postoperatively and transferred on the stereotactic MET-PET and FDG-PET using a local implementation of the PET processing software.

As previously described (*18*), we evaluated radioactive content in noninvolved gray matter using ROIs delineated in the frontal and temporal cortex of the hemisphere contralateral to the tumor. We calculated the mean counting rates in the ROIs distributed in the cortex. These mean counting rates were weighted for the number of pixels in each ROI and used to calculate tumor-to-cortex ratios.

A total of 93 cylindrical tumor biopsy specimens (diameter = 1 mm, length = 1 cm) were obtained from the serial stereotactic biopsies performed with a side-cutting cannula after the technique described by Kelly et al. (*19*). After formalin-fixation and embedding, serial sections were obtained and stained with hematoxylin and eosin, Masson's trichrome and some immunostains (glial fibrillary acidic protein, S-100 protein, neuron-specific enolase, vimentin and others) when necessary (*20*). Presence or absence of nonexclusive histologic features were recorded in all samples: infiltrating tumor cells in brain tissue surrounding a tumor, anaplasia, focal microscopic necrosis and extensive microscopic necrosis.

Statistical analysis involved Spearman correlation coefficient, Kruskal-Wallis test and Mann-Whitney U-test without correction for multiple comparisons.

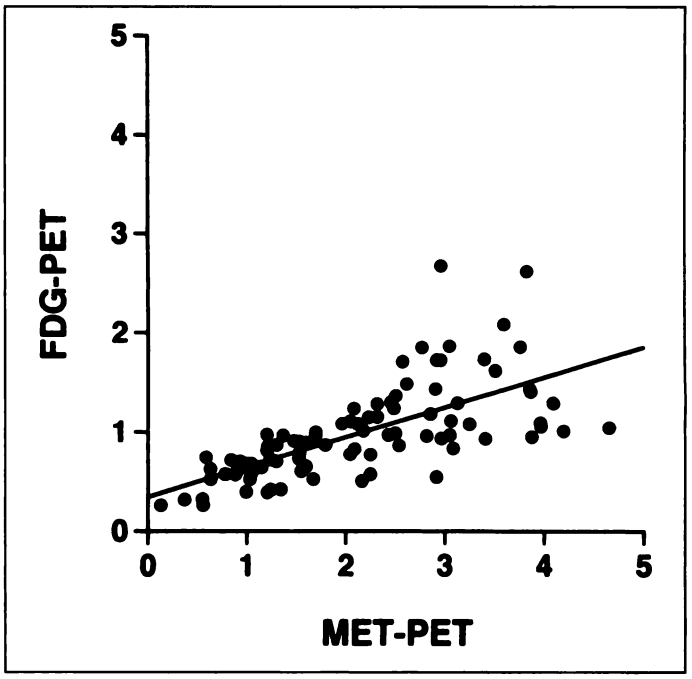

FIGURE 1. Relationship between the uptake of ^{11}C-MET (x axis) and ^{18}F-FDG (y axis) expressed as tumor-to-cortex ratios at the level of 93 stereotactic samples where tumor tissue is demonstrated histologically (Spearman rho = 0.77, $p < 0.0001$). The equation of the linear regression is $y = 0.3x + 0.35$.

RESULTS

In the total set of 93 tumor samples, tumor-to-cortex ratios calculated on MET-PET and FDG-PET were highly positively correlated (Fig. 1, Spearman rho = 0.77, $p < 0.0001$).

The tumor samples were divided into three categories in function of histologic characteristics: samples with typical anaplastic changes (n = 63), samples from nonanaplastic areas

TABLE 2
Relative Uptake of Carbon-11-Methionine and Fluorine-18-FDG at the Level of Tumor Samples with Different Histologic Features (mean ± s.d.)*

	Anaplastic samples	Nonanaplastic samples	Infiltrating cells in brain tissue	Kruskal-Wallis
^{11}C-MET	2.51 ± 1.00	1.35 ± 0.70†	1.38 ± 0.75‡	$p < 0.0001$
^{18}F-FDG	1.13 ± 0.49	0.66 ± 0.30†	0.76 ± 0.20§	$p < 0.0001$

*Values calculated as tumor over cortex ratios.
†Mann-Whitney U-test: different from anaplastic samples ($p < 0.0001$).
‡Mann-Whitney U-test: different from anaplastic samples ($p < 0.0005$).
§Mann-Whitney U-test: different from anaplastic samples ($p < 0.005$).

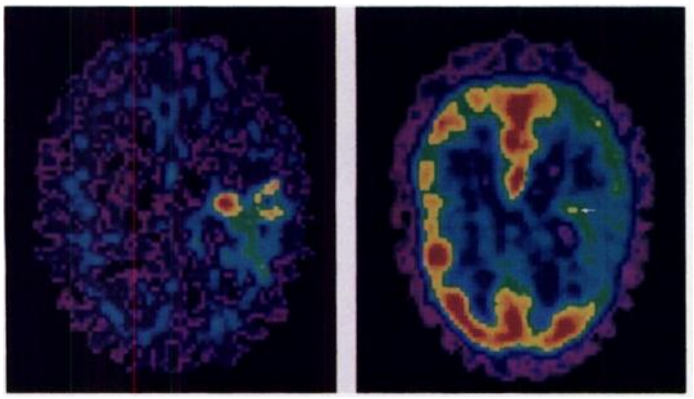

FIGURE 2. Fluorine-18-FDG (left) and ^{11}C-MET (right) PET images of an anaplastic astrocytoma in the temporal lobe. The uptake of ^{18}F-FDG is globally reduced in the tumor area, but a spot of high ^{18}F-FDG uptake is found where stereotactic histologic samples demonstrate anaplasia (arrow). The uptake of ^{11}C-MET is the most pronounced at the level of this anaplastic area, but increased uptake of this tracer is also found in nonanaplastic zones of the tumor.

of the tumor (n = 19) and samples with only infiltrating tumor cells in brain tissue (n = 13). The three categories of samples had significantly different values of tumor-to-cortex ratios calculated on MET-PET (Kruskal-Wallis, $p < 0.0001$). Similar differences between samples from the three categories were also found on FDG-PET (Table 2). In both MET-PET and FDG-PET, these differences were due to the higher values at the level of anaplastic samples compared to nonanaplastic samples and samples with infiltrating tumor cells. Levels of tracer uptake relative to the cortex were different for MET-PET and FDG-PET. The mean tumor-to-cortex ratio was higher than one in all three groups of tumor samples for MET-PET but only in the group of anaplastic samples for FDG-PET. Figure 2 illustrates the higher uptake of both tracers in the anaplastic area of the tumor in a patient with anaplastic astrocytoma. This case also illustrates the presence of elevated uptake of ^{11}C-MET in nonanaplastic areas of the tumor where ^{18}F-FDG appears reduced relatively to the cortex.

Presence of focal or extensive necrosis at the level of anaplastic samples significantly reduced tumor-to-cortex ratios calculated on MET-PET (Kruskal-Wallis, $p < 0.005$). Such a significant effect of necrosis was not found on FDG-PET, even if lower values in the few samples with extensive necrosis were noticed (Table 3). When samples with focal and extensive necrosis were grouped in the statistical analysis, tumor-to-cortex ratios were significantly lower at the level of samples

TABLE 3
Relative Uptake of Carbon-11-Methionine and Fluorine-18-FDG at the Level of Anaplastic Samples with or without Necrosis (mean ± s.d.)*

	No necrosis (n = 48)	Focal necrosis (n = 8)	Extensive necrosis (n = 4)	Kruskal-Wallis
^{11}C-MET	2.72 ± 0.90	1.84 ± 1.10†	1.20 ± 0.36‡	$p < 0.005$
^{18}F-FDG	1.16 ± 0.44	1.12 ± 0.75	0.74 ± 0.18	ns

*Values calculated as tumor over cortex ratios.
†Mann-Whitney U-test: different from samples without necrosis ($p < 0.05$).
‡Mann-Whitney U-test: different from samples without necrosis ($p < 0.005$).
ns = not significant.

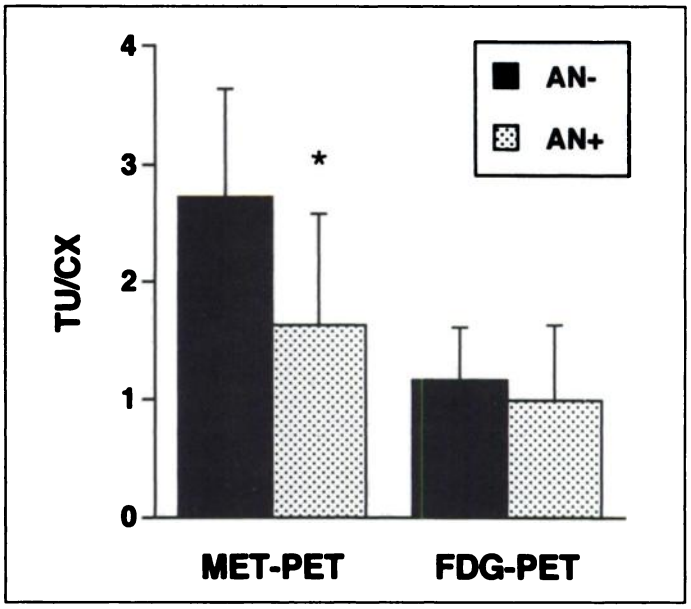

FIGURE 3. Mean tumor-to-cortex ratios (TU/CX) for ^{11}C-MET (MET-PET) and ^{18}F-FDG (FDG-PET) in anaplastic samples with (AN+) and without (AN-) focal or extensive necrosis at pathologic examination (bar = s.d.). Difference between AN+ and AN- is significant for MET-PET (*Mann-Whitney U test, $p < 0.005$) but not for FDG-PET.

with necrosis on MET-PET (Mann-Whitney U test, $p < 0.005$) but not on FDG-PET (Fig. 3).

DISCUSSION

This study shows a correlated increase in ^{11}C-MET and ^{18}F-FDG uptake in anaplastic areas of malignant human gliomas.

The ratio method used for semiquantification of the images generates directly comparable results for the two tracers. Despite the normalization inherent to the method, it does not provide, however, common thresholds of uptake for the two tracers. Indeed, normal gray matter presents a high uptake of FDG while its uptake of methionine is relatively low. Simple relative quantification instead of absolute quantification is justified by previous results obtained in a different series of patients and which has showed that, for ^{18}F-FDG, the simple ratio method is as effective as local glucose metabolic rate calculation for the differentiation between anaplastic and nonanaplastic areas of brain tumors (*21*). Furthermore, some investigations on human brain tumors have refuted assumptions on the lumped constant which corrects for the difference in transport and phosphorylation rates between glucose and ^{18}F-FDG for quantification by autoradiographic and graphical methods (*1,22*). In addition, the actual local glucose concentration in the tumor capillaries, necessary for metabolic rate quantification and estimated from the peripheral arterial plasma level, varies probably regionally in the tumor in function of the local glycolysis stimulation. Similarly, the biochemical mechanisms that govern the uptake of ^{11}C-MET in brain tumors have not been clarified yet, and the methods proposed for the quantification of this uptake doubtfully provide metabolic rates of a single biochemical process (*23,24*). Our study, under histologic control, demonstrates that the uptakes of ^{11}C-MET and ^{18}F-FDG are heterogeneous within the limits of a malignant glioma. The heterogeneity demonstrated in vivo by PET probably represents the metabolic counterpart of the well-known histologic heterogeneity of gliomas (*25*). Similar influence of anaplastic changes on the uptake of the two tracers probably

explains the correlation found between the two uptake ratios in the whole series of tumor samples.

The relationship between local glucose consumption and anaplasia, a major predictor of survival in glial tumors (*26*), probably originates in the abnormal induction of glycolysis in malignant proliferating cells, partly as a consequence of overexpression of glucose transporters (*27,28*). On the other hand, total dependence of ^{11}C-MET uptake on the proliferative activity of human gliomas seems contradicted by the increased uptake demonstrated by PET in various low-grade gliomas (*4–6,29*). Nevertheless, non-CNS tumor models have revealed influence of proliferative activity on methionine uptake which might explain the higher uptake in anaplastic zones in our series of tumor (*30,31*). Furthermore, previous PET studies have revealed higher global ^{11}C-MET uptake in high-grade than in low-grade gliomas (*4–6,29*).

Our analysis is based on a method of PET-guided stereotactic biopsy that we have initially developed and validated with ^{18}F-FDG (*11,14*). This study demonstrates that ^{11}C-MET offers a worthy alternative for the PET guidance of stereotactic diagnostic or therapeutic procedures towards the anaplastic components of the tumor. Compared to ^{18}F-FDG, ^{11}C-MET presents the advantage of a better detection of nonanaplastic tumor zones and of brain regions with infiltrating neoplastic cells. This advantage is valuable when a stereotactic procedure aims at a volumetric resection based on imaging information. Another advantage of ^{11}C-MET compared to ^{18}F-FDG is the more reliable differentiation of tumor from gray matter. Nevertheless, ^{18}F-FDG may remain the tracer of choice to image contrast-enhanced lesions on CT or MRI, since blood-brain barrier alteration has minimal influence on FDG-PET (*1,32,33*) but might interfere with ^{11}C-MET uptake (*23,24,34*).

We observe a reduction in ^{11}C-MET but not ^{18}F-FDG uptake at the level of tumor areas with necrotic components. This observation parallels recent microautoradiographic results on animal non-CNS cancer models showing that uptake of ^{14}C-labeled methionine is proportional to the amount of viable tumor cells and is low in macrophages and other non-neoplastic cellular components (*30*). On the other hand, several microautoradiographic experiments have revealed high uptake of ^{18}F-FDG in tumor-associated macrophages and prenecrotic neoplastic cells (*30,35*). We have previously attributed to the same phenomenon the better survival of patients with glioblastoma in whom a first cycle of chemotherapy induces a hypermetabolic reaction (*18*). This uptake of tracer in cellular components related to the necrotic process might explain our present results of maintained ^{18}F-FDG uptake in anaplastic areas with necrosis.

CONCLUSION

This stereotactic PET study in human gliomas shows parallel anatomical heterogeneity of ^{11}C-MET and ^{18}F-FDG uptakes and influence of anaplastic changes on the uptake of these tracers. Non-neoplastic cellular components are probably implicated in the different influence of necrotic changes in MET-PET and FDG-PET. These results emphasize the complementary role of ^{18}F-FDG and ^{11}C-MET for the study of brain tumors. They support the use of either ^{18}F-FDG or ^{11}C-MET for the stereotactic PET guidance of diagnostic and therapeutic procedures.

ACKNOWLEDGMENTS

This study was supported by grants 9.4503.91 and 9.4513.93F from the Belgian National Lottery and 3.4509.92, 3.4508.92 and 3.4532.94 from the National Funds for Scientific Research, Belgium.

REFERENCES

1. Herholz K, Wienhard K, Heiss WD. Validity of PET studies in brain tumors. *Cerebrovasc Brain Metab Rev* 1990;2:240–265.
2. Coleman RE, Hoffman JM, Hanson MW, et al. Clinical application of PET for the evaluation of brain tumors. *J Nucl Med* 1991;32:616–622.
3. Di Chiro G, DeLaPaz RL, Brooks RA, et al. Glucose utilization of cerebral gliomas measured by ^{18}F-FDG and PET. *Neurology* 1982;32:1323–1329.
4. Bustany P, Chatel M, Derlon JM, et al. Brain tumor protein synthesis and histological grades: a study by PET with ^{11}C-L-methionine. *J Neurooncol* 1986;3:397–404.
5. Derlon JM, Bourdet C, Bustany P, et al. Carbon-11-L-methionine uptake in gliomas. *Neurosurgery* 1989;25:720–728.
6. Ogawa T, Shishido F, Kanno I, et al. Cerebral glioma: evaluation with methionine PET. *Radiology* 1993;186:45–53.
7. Wienhard K, Herholz K, Coenen HH, et al. Increased amino acid transport into brain tumors measured by PET of L-(2-^{18}F)fluorotyrosine. *J Nucl Med* 1991;32:1338–1346.
8. Bergstrom M, Collins VP, Ehrin E, et al. Discrepancies in brain tumor extent as shown by computed tomography and PET using ^{68}Ga-EDTA, ^{11}C-glucose and ^{11}C-methionine. *J Comput Assist Tomogr* 1983;7:1062–1066.
9. Tovi M, Lilja A, Bergstrom M, et al. Delineation of gliomas with magnetic resonance imaging using Gd-DTPA in comparison with computed tomography and PET. *Acta Radiology* 1990;31:417–429.
10. Herholz K, Pietrzyk U, Voges J, et al. Correlation of glucose consumption and tumor cell density in astrocytomas: a stereotactic PET study. *J Neurosurg* 1993;79:853–858.
11. Levivier M, Goldman S, Bidaut LM, et al. PET-guided stereotactic brain biopsy. *Neurosurgery* 1992;31:792–797.
12. Thomas DGT, Gill SS, Wilson C. Current and future utilization of PET scanning in the evaluation and management of malignant cerebral glioma. In: M.L.J. Appuzzo, ed. *Malignant cerebral glioma*. Park Ridge, IL: American Association of Neurological Surgeons 1991;79–89.
13. Maciunas RJ, Kessler RM, Maurer C, et al. PET imaging directed stereotactic neurosurgery. *Stereotact Funct Neurosurg* 1992;58:134–140.
14. Levivier M, Goldman S, Pirotte B, et al. Diagnostic yield of stereotactic brain biopsy guided by PET with ^{18}F-fluorodeoxyglucose. *J Neurosurg* 1995;82:445–452.
15. Comar D, Cartron J-C, Maziere M, Marazano C. Labeling and metabolism of ^{11}C-methioninemethyl. *Eur J Nucl Med* 1976;1:11–14.
16. Dethy S, Goldman S, Blecic S, et al. Carbon-11-methionine and ^{18}F-FDG PET study in brain hematoma. *J Nucl Med* 1994;35:1162–1166.
17. Hamacher K, Coenen HH, Stöcklin G. Efficient stereospecific synthesis of no-carrier-added 2-[^{18}F]fluoro-2-deoxy-D-glucose using aminopolyether supported nucleophilic substitution. *J Nucl Med* 1986;27:235–238.
18. De Witte O, Hildebrand J, Luxen A, Goldman S. Acute effect of carmustine on glucose metabolism in brain and glioblastoma. *Cancer* 1994;74:2836–2842.
19. Kelly PJ, Daumas-Duport C, Kispert DB, et al. Imaging-based stereotactic serial biopsies in untreated intracranial glial neoplasms. *J Neurosurg* 1987;66:865–874.
20. Brucher J-M. Neuropathological diagnosis with stereotactic biopsies. Possibilities, difficulties and requirements. *Acta Neurochir (Wien)* 1993;124:37–39.
21. Goldman S, Levivier M, Pirotte B, et al. Regional glucose metabolism and histopathology of gliomas: a study based on positron emission tomography-guided stereotactic biopsy. *Cancer* 1996;78:1098–1106.
22. Junck L, McKeever PE, Ross DA, et al. The significance of fluorodeoxyglucose uptake in gliomas [Abstract]. *J Cereb Blood Flow Metab* 1995;15:S737.
23. Meyer G-J, Van den Hoff J, Burchert W, Hundeshagen H. Approaches to quantitative analysis of amino acid transport and metabolism. In: Mazoyer BM, Heiss WD and Comar D, eds. *PET studies on amino acid metabolism and protein synthesis*. Dordrecht: Kluwer Academic Publishers; 1993:183–196.
24. Ishiwata K, Kubota K, Murakami M, et al. Re-evaluation of amino acid PET studies: can the protein synthesis rates in brain and tumor tissues be measured in vivo? *J Nucl Med* 1993;34:1936–1943.
25. Paulus W, Peiffer J. Intratumoral histologic heterogeneity of gliomas: a quantitative study. *Cancer* 1989;64:442–447.
26. Daumas-Duport C, Scheithauer BW, O'Fallon J, Kelly PJ. Grading of astrocytomas: a simple and reproductible method. *Cancer* 1988;62:2152–2165.
27. Warburg O. In: *The metabolism of tumors*. London: Arnold Constable 1930;75–327.
28. Yamamoto T, Seino Y, Fukomoto H, et al. Overexpression of facilitate glucose transporter genes in human cancer. *Biochem Biophys Res Commun* 1990;170:223–230.
29. Mosskin M, von-Holst H, Bergstrom M, et al. PET with ^{11}C-methionine and computed tomography of intracranial tumors compared with histopathologic examination of multiple biopsies. *Acta Radiol* 1987;28:673–681.
30. Kubota R, Kubota K, Yamada S, et al. Methionine uptake by tumor tissue: a microautoradiographic comparison with FDG. *J Nucl Med* 1995;36:484–492.
31. Miyazawa H, Arai T, Iio M, Hara T. PET imaging of non-small-cell lung carcinoma with carbon-11-methionine: relationship between radioactivity uptake and flow-cytometric parameters. *J Nucl Med* 1993;34:1886–1891.
32. Hawkins RA, Phelps ME, Huang SC. Effects of temporal sampling, glucose metabolic rates and disruptions of the blood-brain barrier on the FDG model with and without a vascular compartment: studies in human brain tumors with PET. *J Cereb Blood Flow Metab* 1986;6:170–183.
33. Herholz K, Rudolf J, Heiss WD. FDG transport and phosphorylation in human gliomas measured with dynamic PET. *J Neurooncol* 1992;12:159–165.
34. Roelcke U, Radü EW, Leenders KL. Carbon-11-methionine and ^{82}Rb uptake in human brain tumors: comparison of carrier dependent blood-brain barrier transport. In: Mazoyer BM, Heiss WD and Comar D, eds. *PET studies on amino acid metabolism and protein synthesis*. Dordrecht: Kluwer Academic Publishers; 1993;197–199.
35. Kubota R, Yamada S, Kubota K, et al. Intratumoral distribution of fluorine-18-fluorodeoxyglucose in vivo: high accumulation in macrophages and granulation tissues studied by microautoradiography. *J Nucl Med* 1992;33:1972–1980.